Direct Effective Power Control (D-EPC) for LLC Resonant Converters Operating in Boost Mode Using Event-Driven-Timer Based Digital Controller

Yuto Yoshimura
Graduate school of environmental, life, natural science and technology
Okayama University
Okayana, Japan
pqx88wuy@s.okayama-u.ac.jp

Kenji Funatani
System Solutions Engineering HQ
ROHM Co., Ltd.
Yokohama, Japan
Kenji.Funatani@dsn.rohm.co.jp

Kazuhiro Umetani
Graduate school of environmental, life, natural science and technology
Okayama University
Okayana, Japan
umetani@okayama-u.ac.jp

Toshiyuki Zaitsu
LSI Business Unit
ROHM Co., Ltd.
Yokohama, Japan
toshiyuki.zaitsu@rohm.co.jp

Akito Nakagaki
Graduate school of environmental, life, natural science and technology
Okayama University
Okayana, Japan
pr3g4r2e@s.okayama-u.ac.jp

Masataka Ishihara
Graduate school of environmental, life, natural science and technology
Okayama University
Okayana, Japan
masataka.ishihara@s.okayama-u.ac.jp

Eiji Hiraki
Graduate school of environmental, life, natural science and technology
Okayama University
Okayana, Japan
hiraki@s.okayama-u.ac.jp

***Abstract*—The LLC converter is a topology using resonance and is effective for miniaturization and high efficiency. Generally, LLC converters use a direct frequency control (DFC) method, which has the issue of slow transient response characteristics. Therefore, power factor control (called previously), which directly controls the effective power (D-EPC) of the resonant circuit in LLC, has been proposed previously. However, it has been adopted only in series resonant operation (buck mode) because the magnetizing inductance was not considered. In this paper, a small-signal characteristics considering the effect of magnetizing inductance is derived, showed that D-EPC is effective even in boost mode, and confirm the characteristics by experiments**

Keywords—LLC converter, power factor, stability, digital control

I. Introduction

The LLC converter is a topology that uses resonance, enabling high efficiency operation at high frequencies. The high-frequency drive also enables miniaturization of passive components. Because of these features, research to replace conventional buck converters with LLC converters was promoted [1]-[5]. However, it has become difficult to have apply LLC converter to point-of-load (PoL) converter which, require stability against sudden load fluctuations [6][7]. This is due to the LLC converter is conventionally controlled by direct frequency control (DFC) using a voltage-controlled-oscillator (VCO). In the case of DFC, the dynamic characteristics of the LLC converter vary significantly depending on the load condition [8][9]. As a result, fast response to load changing is difficult. As previous study, There are many challenges to overcome this drawback of DFC [12]-[19].

Among them, power factor control (called previously) [12]-[14] is promising for fast response of LLC converters because small-signal characteristics with little load dependence have been revealed. This method controls the phase difference between the voltage and current waveform in the resonant circuit. Therefore, it is a method of direct-effective power control (D-EPC) that adjusts the power factor of the resonant circuit. However, the derivation of the small-signal characteristics of D-EPC ignores the effect of the magnetizing inductance in the previous study [12]-[14]. Thus, it could not be used in the boost mode that is commonly used in the LLC converter applications.

In this paper, the small-signal characteristics of D-EPC considering magnetizing inductance are derived from the power-focused equation of state to show the effectiveness of the control characteristics and the adaptability of D-EPC in boost mode. The remainder of this paper consists of five sections. Section II briefly describes the shortcomings of conventional control and the control method of D-EPC. Next, in Section III, we propose a method to analyze the small-signal characteristics of the D-EPC considering the magnetizing inductance. In Section IV, we confirm the validity of the proposed analysis method by conducting actual measurements of the control characteristics. Finally, conclusions are presented in Section V.

II. Principle of D-EPC

A. Review of Convetinaol contorol (DFC)

Fig.1 shows LLC converter with direct frequency control DFC using VCO. Here, Q_1 is the high-side switch, Q_2 is the low-

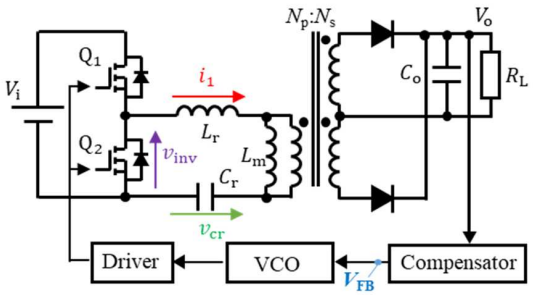

Fig.1. Block diagram of LLC using VCO

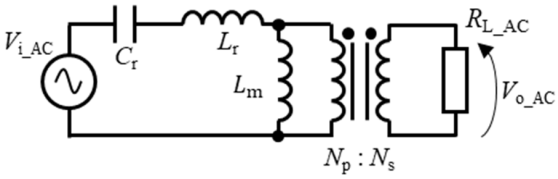

Fig.2. Equivalent circuit of LLC converter using FHA.

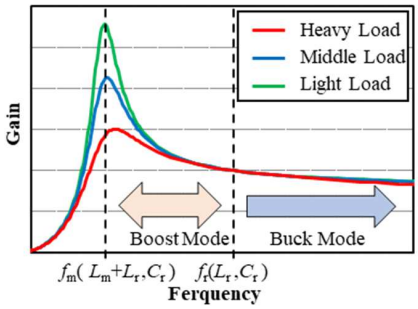

Fig.3. Frequency vs gain characteristic LLC

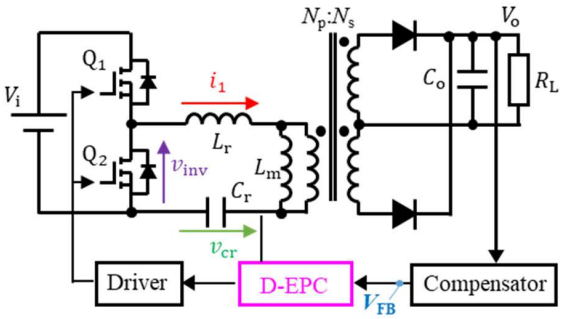

(a) Block diagram of LLC using D-EPC

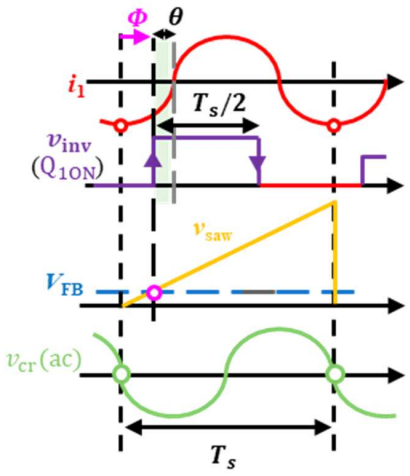

(b) Timing chart of D-EPC

Fig.4. The principle of operation of D-EPC for LLC converter

side switch, L_m of the transformer is magnetizing inductance, L_r is the resonant inductance, C_r is the resonant capacitor, C_o is the smoothing capacitor and R_L is the load resistance. f_s is the operating frequency.Fig.2 shows the equivalent circuit of the LLC converter based on the FHA (Fundamental Harmonics Analysis) method. Using Fig.2, the frequency versus gain characteristic is expressed by (1)

$$\frac{V_{o\_AC}}{V_{i\_AC}} = \frac{1}{\sqrt{\left(1+\frac{1}{S}-\frac{1}{SF^2}\right)+Q^2\left(F-\frac{1}{F}\right)^2}} \quad (1)$$

$$S=\frac{L_m}{L_r}, f_r=\frac{1}{2\pi\sqrt{L_rC_r}}, F=\frac{f_s}{f_r}, Z_r=\sqrt{\frac{L_r}{C_r}}$$

$$N=\frac{N_p}{N_s}, R_{L\_AC}=\frac{8}{\pi^2}N^2R_L, Q=\frac{Z_r}{R_{L\_AC}}$$

As shown in (1), the LLC converter can control the output voltage by adjusting the operation frequency f_s. Fig.3 shows the gain versus frequency characteristics of the LLC converter. Fig.3 shows that the characteristic of gain and frequency depends on the load. Therefore, conventional control (DFC) using VCO is difficult to control design because the transfer function of the plant is highly load-dependent. On the other hand, D-EPC has a small load dependence and is easy to control design.

B. Operation of D-EPC[13][14]

D-EPC (previously called "power factor control") method regulates the output voltage by adjusting the angle θ which is defined as the phase difference between the inverter voltage v_{inv} and the primary resonant current i_1. Fig 4(a) shows the block diagram of D-EPC and Fig.4 (b) the timing chart. Here, V_{saw} is the saw wave of the control circuit, V_{FB} is the feedback voltage, Q_{1on} is the turn-on signal of the high-side switch Q_1, and ϕ is the phase difference from zero crossing of the resonant capacitor to turning on the high-side switch. D-EPC algorithm generates V_{saw} with respect to the zero crossing point of the resonant capacitor voltage V_{cr} instead of detecting the current phase, as shown in Fig.4. Then, the switch Q_1 is turned on at the timing, when it crosses V_{FB} to control the phase difference ϕ between the inverter voltage v_{inv} and the primary resonant current i_1. The phase difference ϕ is related to the power factor cosθ by the (2).

$$\cos\theta = \cos(90-\phi) \quad (2)$$

From the relationship in(2), the effective power output by the inverter is controlled based on the power factor cosθ.

Identify applicable funding agency here. If none, delete this text box.

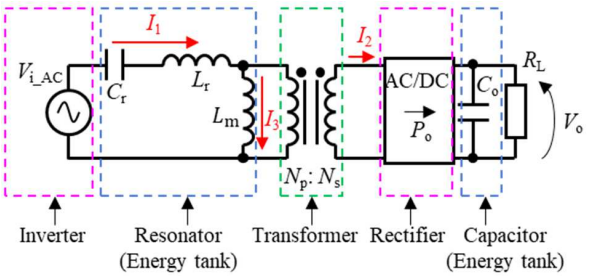

Fig.5. Proposed analysis model for LLC converter

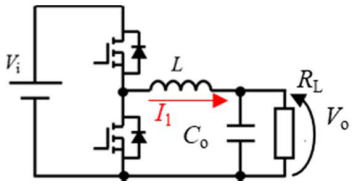

Fig.6. Buck converter

C. *Small signal analysis in buck mode[12]*

The small-signal characteristic analysis establishes equations for the effective-power flow from the inverter to the load resistor in reference [12]. Fig.5 shows an analysis model of LLC converter. In this model, the input voltage is approximated as only Fundamental wave and the rectifier circuit is considered as a lossless power conversion circuit. V and I is root-mean-square value of the voltage and current in each part. V_{i_AC} and V_{o_AC} values are expressed as follows.

$$V_{i\_AC} = \frac{\sqrt{2}}{\pi} V_i \tag{3}$$

$$V_{o\_AC} = \frac{2\sqrt{2}}{\pi} V_o \tag{4}$$

In this case, the effective input power P_i, output power P_{tr} from the secondary winding of the transformer per unit time can be expressed as follows

$$P_i = I_1 V_{i\_AC} \cos\theta \tag{5}$$

$$P_{tr} = I_2 \cdot V_{o\_AC} \tag{6}$$

In the case of the LLC converter in buck mode the LLC converter is used in buck mode, the magnetizing inductance L_m should be large. Therefore, the value of the magnetizing current I_3 is smaller than the secondary current I_2, thus the secondary current I_2 is expressed as

$$I_2 = NI_1 \tag{7}$$

Assuming that the LC resonator is driven at its resonant frequency f_r, the stored energy in the resonator E_{res} during the period of AC voltage is considered to be almost constant. Here, Note that the instantaneous AC voltage of C_r is zero at the instant of peak current in L_r, E_{res} can be formulated as

$$E_{res} = \frac{1}{2} L_r \left(\sqrt{2} I_1\right)^2 \tag{8}$$

The difference between P_{in} and P_{tr} indicates the energy stored in the LC resonator per unit time. Therefore, from (5)-(8), the equation of state for I_1 is expressed as

$$\frac{dE_{res}}{dt} = P_i - P_{tr} \tag{9}$$

$$\therefore \frac{d}{dt}\left\{\frac{1}{2} L_r \left(\sqrt{2} I_1\right)^2\right\} = I_1 V_{i\_AC} \cos\theta - NI_1 \cdot V_{o\_AC} \tag{10}$$

Next, deriving the expression for V_o from V_{o_ac}, the dc output power per unit time P_o of the LLC converter is expressed as

$$P_o = \frac{V_o^2}{R_L} \tag{11}$$

Noting that P_{tr} indicates the ac power per unit time supplied to the rectifier, P_{tr}–P_o can be interpreted as the energy charged in the output smoothing capacitor per unit time. If E_{cap} denotes the total energy stored in the output smoothing capacitor, E_{cap} can be expressed as

$$E_{cap} = \frac{1}{2} C_o V_o^2 \tag{12}$$

Therefore, from (6), (11) and (12), the equation of state for V_{out} is expressed as

$$\frac{dE_{cap}}{dt} = P_{tr} - P_o \tag{13}$$

$$\therefore \frac{d}{dt}\left(\frac{1}{2} C_o V_o^2\right) = NI_1 \cdot V_{o\_AC} - \frac{V_o^2}{R_L} \tag{14}$$

Finally, from (10) and (14), "state-space-equation" of LLC Power Factor Control is derived as follows.

$$\frac{d}{dt}\begin{bmatrix} I_1 \\ V_o \end{bmatrix} = \begin{bmatrix} 0 & -\frac{\sqrt{2}N}{\pi L_r} \\ \frac{2\sqrt{2}N}{\pi C_o} & -\frac{1}{C_o R_L} \end{bmatrix} \begin{bmatrix} I_1 \\ V_o \end{bmatrix} + \begin{bmatrix} \frac{\sqrt{2}N}{\pi L_r} \\ 0 \end{bmatrix} \frac{V_i}{2N} \cos\theta \tag{14}$$

On the other hand, Back converter (Fig.6) is well known "state-space equation" is expressed as

$$\frac{d}{dt}\begin{bmatrix} I_1 \\ V_o \end{bmatrix} = \begin{bmatrix} 0 & -\frac{1}{L} \\ \frac{1}{C_o} & -\frac{1}{C_o R_L} \end{bmatrix} \begin{bmatrix} I_1 \\ V_o \end{bmatrix} + \begin{bmatrix} \frac{1}{L} \\ 0 \end{bmatrix} V_i D \tag{15}$$

Comparing (14) and (15), it is found that they have the same form. Therefore, the method that directly controls the effective power based on the power factor cosθ (D-EPC) has the same control characteristics as the buck converter. This allows the compensator design method of the buck converter to be adapted and enables a faster response.

III. SMALL SIGNAL CHARACTERISTICS IN BOOST MODE

A. *Derivation of Small-Signal Model*

Similar to the buck mode, the small-signal characteristics in the boost mode are also derived by using (9) and (13), which focus on the effective power. However, in the boost mode, the equation is derived by considering the effect of the magnetizing current I_3, which was ignored in (7) in the buck mode.

Since the rectifier circuit is a power load, it can be considered a resistive load. Therefore, the magnetizing current I_3 and the transformer secondary current I_2 are orthogonal. Therefore, the transformer secondary current I_2 is expressed as

$$I_2 = \sqrt{I_1^2 - I_3^2} = \sqrt{I_1^2 - \left(\frac{V_{o\_AC}}{\omega L_m}\right)^2} \tag{16}$$

From (16), which considering the magnetizing current, the equations of state (9) and (13) are expressed once again

$$\frac{d}{dt}\left\{\frac{1}{2}L_r\left(\sqrt{2}I_1\right)^2\right\} = I_1 V_{i\_AC}\cos\theta - N\sqrt{I_1^2 - \left(\frac{V_{o\_AC}}{\omega L_m}\right)^2}\cdot V_{o\_AC} \tag{17}$$

$$\frac{d}{dt}\left(\frac{1}{2}C_o V_o^2\right) = N\sqrt{I_1^2 - \left(\frac{V_{o\_AC}}{\omega L_m}\right)^2}\cdot V_{o\_AC} - \frac{V_o^2}{R_L} \tag{18}$$

Then the small signal transfer function from $\cos\theta$ to V_o derive from (17)(18) to (19).

$$\frac{\delta V_o}{\delta\cos\theta} = \frac{\frac{1}{\eta N}V_i}{2L_r C_o s^2 + \left(C_o\left(1-\eta^2\right)R_L + \frac{2L_r}{R_L\eta^2}\right)s + 1} \tag{19}$$

where η is the ratio of transformer primary current I_1 and secondary current I_2 in steady state as shown in (20)

$$\eta = \frac{NI_2}{I_1} = \frac{\omega L_m}{\sqrt{R_{L\_AC}{}^2 + \omega^2 L_m{}^2}}, \quad \eta = \frac{\omega L_m}{\sqrt{R_{L\_AC}{}^2 + \omega^2 L_m{}^2}} \tag{20}$$

On the other hand, it is well known that the buck converter (Fig.6) can be linearly controlled and the small-signal characteristic is expressed by (21).

$$\frac{\delta V_o}{\delta D} = \frac{V_i}{LC_o s^2 + \frac{L}{R_L}s + 1} \tag{21}$$

Comparing (19) and (21), we can see that both are second-order delay systems and that the corner frequency is constant. It also shows that the damping factor depends on the load. Therefore, the LLC converter in boost mode has the same control characteristics as the buck converter by controlling the effective power based on $\cos\theta$.

B. *Calculating plant transfer function*

Fig. 7 shows the calculation characteristic the plant (control to output) transfer function at R_o=1.6Ω and 4.7Ω based on (19), and the values of TABLE.I were used for each parameter. Fig.7 shows that there is no increase in gain at the resonance frequency regardless of the load condition. This is due to the effect of the magnetizing inductance, which tends to increase the damping coefficient. This effect causes the separation of the poles, resulting in a Bode plot similar to that of a first-order system. It can also be seen that the pole separation increases with light load. This model is considered to be a light load increases the attenuation coefficient by increasing the value of η in (19) .

IV. Imprimentation and Experiments

A. *Imprimentation and Operating Mechanism*

Fig.8 shown circuit diagram. This circuit consists of an LLC converter main circuit, a capacitor voltage detection circuit, a saw wave circuit, and a digital controller. The digital controller is the ML62Q203x/4x (16-bit, 16 MHz clock, 64 MHz timer)[20]. This controller can realize event-driven operation

TABLE.I Calculation parameters

Parameter	Symbol	Value
DC input Voltage	V_{in_DC}	48[V]
Regulated Output Voltage	V_o	12[V]
Transformer turn-ratio	N	2
Series resonant inductance	L_r	2[μH]
Magnetizing inductance	L_m	7[μH]
Resonant capacitance	C_r	500[nF]
Output capacitance	C_o	350[μF]

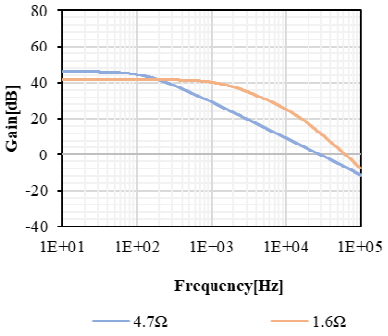

(a) Gain characteristics

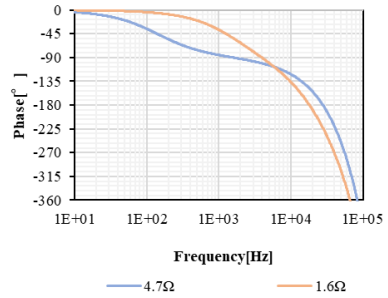

(b) Phase characteristics

Fig.7. Calculation result (control to output bode plot)

without CPU control, and the timer has a frequency tracking function with an internal comparator.

Fig.9 shows the timing chart. The control method is based on the saw wave as in the D-EPC operation. The ON period of the switch is determined by a timer in the digital controller. In this circuit, the rising edge of the internal comparator CMP_{tr} is used as an event, and frequency tracking is performed from the previous resonance period to the triangular wave timer for phase delay timing adjustment.

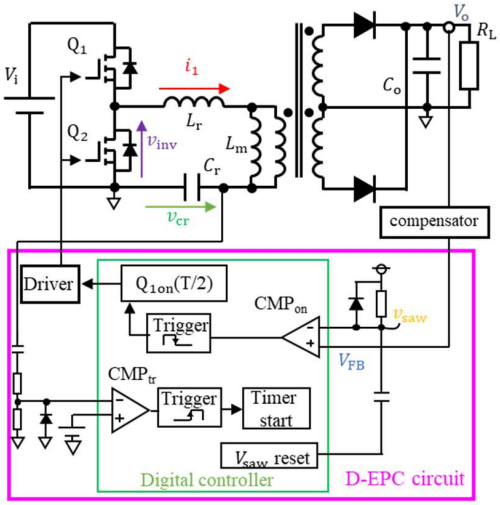

Fig.8. Circuit Diagram of LLC D-EPC

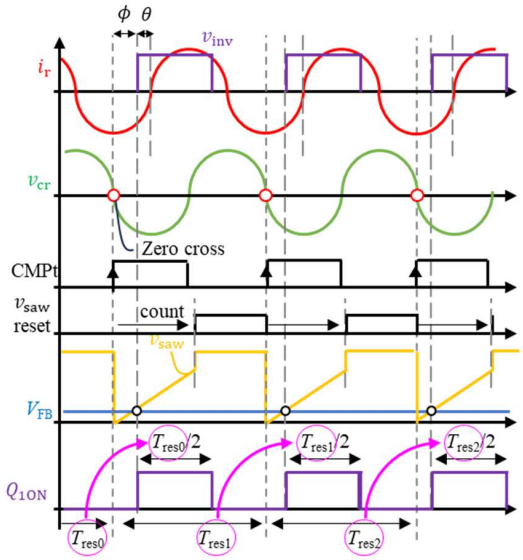

Fig.9. Timing chart of LLC D-EPC

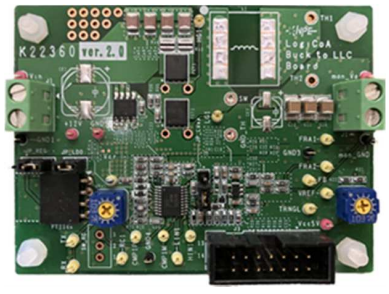

Fig.10. Prototype board of LLC D-EPC

B. *Experiments*

Fig.10 shows the prototype board. The experiment also used Table.I for each parameter. This circuit is stepped down from 48 V to 12V. The maximum output current is 8 A and the maximum output power is 100 W. The series resonance frequency is 150 kHz. In the experiment, the feedback voltage V_{FB} is VFB is applied externally, and the circuit is operated in open loop. Here, the feedback voltage is adjusted so that the output voltage is 12 V.

Fig.11 shows actual operating waveform with load resistance of 4.7Ω. The current waveforms in Fig.11 show that the LLC converter is operating at a frequency lower than the resonant frequency, to operate in boost mode. The high-side switch Q1 turns on at the point where the feedback voltage and the saw wave intersect. Therefore, it was found that D-EPC circuit operates even in the boost mode and can be adapted to all modes of operation.

C. *Measuring plant transfer function*

Fig. 12 shows the measured plant transfer function at R_o=1.6Ω and 4.7Ω. From Fig. 12, the transfer function shows the same characteristics as calculation result of proposed model. From this result, it can be said that the small-signal characteristics in (19) sufficiently predict damping factor. The characteristics of LLC converters using D-EPC are similar to those of buck converters.. This indicates that it is possible to adapt the compensator design of the buck converter to the LLC converter using D-EPC.

V. CONCULTION

Direct effective power control(D-EPC) method for LLC control was proposed. A small-signal characteristic of the plant transfer function (control to output) considering magnetizing inductance for the boost mode operation was derived from “power -focused equation of state”. Test board was implemented and evaluated at Vin=48V, V_{out}=12V, R_o=1.6 Ω and 4.7Ω. As a result, D-EPC LLC

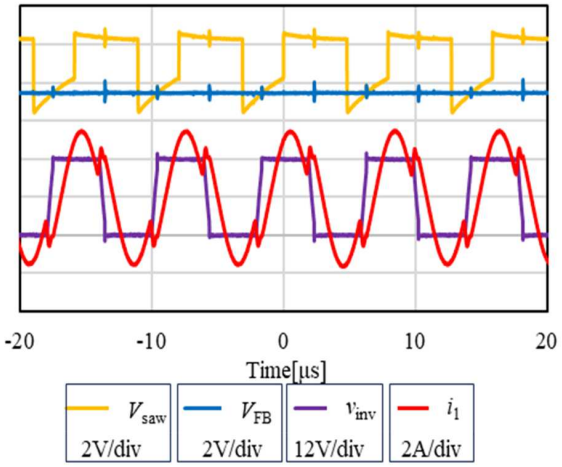

Fig.11. Operating wave form

converter in boost mode was working properly and "the plant transfer function" was in good agreement between calculated and measured bode-plot. It is confirmed that D-EPC method is effective even in the boost mode.

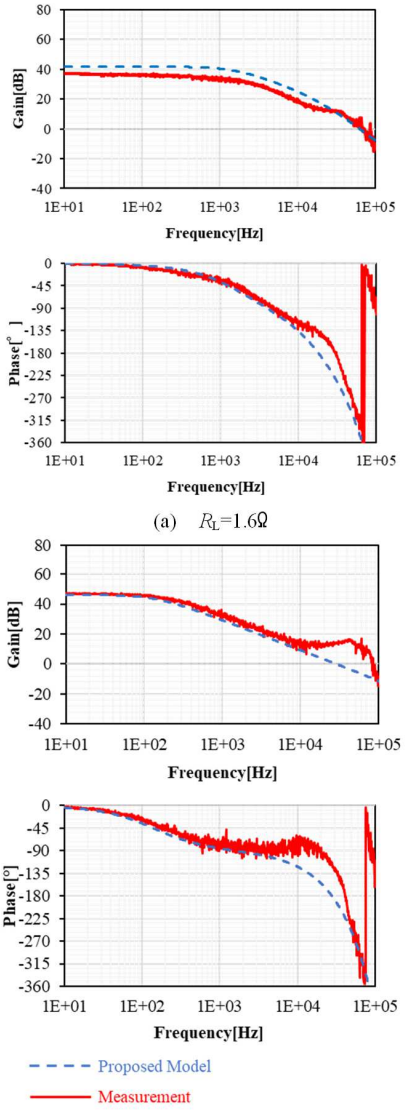

(a) R_L=1.6Ω

(b) R_L=4.7Ω

Fig.12. Experimental result (control to output bode plot)

REFERENCES

[1] G. Yang, P. Dubus, and D. Sadarnac, "Double-phase highefficiency,wide load range high- voltage/low-voltage LLC DC/DC converter forelectric/hybrid vehicles," IEEE Trans. Power Electron., vol. 30, no. 4,pp. 1876-1886, Apr. 2015.

[2] C. Duan, H. Bai, W. Guo, and Z. Nie, "Design of a 2.5-kW 400/12Vhigh-efficiency DC/DC converter using a novel synchronous rectification control for electric vehicles," IEEE Trans. Transportation Electrification, vol. 1, no. 1, pp. 106-114, Jun. 2015.

[3] J.-B. Lee, J.-K. Kim, J.-H. Kim, J.-I. Baek, and G.-W. Moon, "A high efficiency PFM half-bridge converter utilizing a half-bridge LLC converter under light load conditions," IEEE Trans. Power Electron., vol. 30, no. 9, pp. 4931-4942, Sept. 2015.

[4] C. Fei, R. Gadelrab, Q. Li, and F. C. Lee, "High-frequency three-phase interleaved LLC resonant converter with GaN devices and integrated planar magnetics," IEEE J. Emerg. Select. Topics Power Electron., vol. 7, no. 2, pp. 653-663, Jun. 2019.

[5] R. Beiranvand, B. Rashidian, M. R. Zolghadri, and S. M. H. Alavi, "A design procedure for optimizing the LLC resonant converter as a wide output range voltage source," IEEE Trans. Power Electron., vol. 27, no. 8, pp. 3749-3763, Aug. 2012.

[6] C.-O Yeon, J.-W. Kim, M.-H. Park, I.-O. Lee, and G.-W. Moon, " Improving the light-load regulation capability of LLC series resonant converter using impedance analysis," IEEE Trans. Power Electron., vol. 32, no. 9, pp. 7056-7067, Sept. 2017.

[7] Z. Fang, J. Wang, R. Liu, L. Xiao, J. Zhang, G. Hu, and Q. Liu, "Energy feedback control of light-load voltage regulation for LLC resonant converter," IEEE Trans. Power Electron., vol. 34, no. 5, pp. 4807-4819, May 2019.

[8] H.-P. Park and J.-H. Jung, "Power stage and feedback loop design for LLC resonant converter in high-switching-frequency operation," IEEE Trans. Power Electron., vol. 32, no. 10, pp. 7770-7782, Oct. 2017.

[9] M. F. Menke, A. R. Seidel, and R. V. Tambara, "LLC LED driver small-signal modeling and digital control design for active ripple compensation," IEEE Trans. Ind. Electron., vol. 66, no. 1, pp. 387-396, Jan. 2019.

[10] Z. Fang, J. Wang, S. Duan, K. Liu, and T. Cai, "Control of an LLC resonant converter using load feedback linearization," IEEE Power Electron., vol. 33, no. 1, pp. 887-898, Jan. 2018.

[11] S. Tian, F. C. Lee, Q. Li, "Equivalent Circuit Modeling of LLC Resonant Converter," IEEE Transactions on Power Electronics, Vol. 35, No.8, pp.8833-8845, Aug. 2020.

[12] K.Umetani, K. Shimomura, K. Yamada, T. Kawakami, M. Ishihara, and E. Hiraki, "A Control Method Based on Power Factor for Improving Output Voltage Stability and Efficiency of LLC Converter in Wide Range of Output Voltage and Load Impedance," IEEE ECCE 2021, pp.3436-3443.

[13] K. Yamada, K. Umetani, E. Hiraki, and M. Ishihara, "Phase-Shift Based on Power Factor Control for LLC Converter with High Output Stability Against Load Fluctuation," IEEE Southern Power Electronics Conference (SPEC), 2022.

[14] T. Zaitsu, Y. Yoshimura, K. Umetani, M. Ishihara, E. Hiraki and K. Horii, "Compact Hardware Implementation of Power Factor Control for LLC converter with Event-Driven-Timer Based Digital Controller," 2024 IEEE Applied Power Electronics Conference and Exposition (APEC), Long Beach, CA, USA, 2024, pp. 2015-2020

[15] C. Adragna, "Time-shift control of LLC resonant converters" PCIM Europe 2010 Proceedings, Paper #113, Page(s) 661- 666, May 2010.

[16] C. Adragna, D. Ciambellotti, M. Dell'Oro and F. Gallenda, "Digital implementation and performance evaluation of a time-shift-controlled LLC resonant half-bridge converter," 2014 IEEE Applied Power Electronics Conference and Exposition - APEC 2014, Fort Worth, TX, USA, 2014, pp. 2074-2080

[17] Z. Hu, Y. -F. Liu and P. C. Sen, "Bang-Bang Charge Control for LLC Resonant Converters," in IEEE Transactions on Power Electronics, vol. 30, no. 2, pp. 1093-1108, Feb. 2015

[18] B. McDonald and Y. Li, "A novel LLC resonant controller with best-in-class transient performance and low standby power consumption," 2018 IEEE Applied Power Electronics Conference and Exposition (APEC), San Antonio, TX, USA, 2018, pp. 489-493

[19] S. S. Shah, U. Raheja and S. Bhattacharya, "Input Impedance Analyses of Charge Controlled and Frequency Controlled LLC Resonant Converter," 2018 IEEE Energy Conversion Congress and Exposition (ECCE), Portland, OR, USA, 2018, pp. 1-5

[20] https://www.rohm.com/products/micon/logicoa/ml62q20xx-series/ml62q2035-nnngd_taping_-product#productDetail